### Title

Subacute nicotine co-exposure has no effect on 2,2′,3,5′,6- pentachlorobiphenyl disposition but alters hepatic cytochrome P450 expression in the male rat




### Authors

Stamou, Marianna
Uwimana, Eric
Flannery, Brenna M
et al.



### Publication Date

2015-12-01

### DOI

10.1016/j.tox.2015.10.002

Peer reviewed

Toxicology 338 (2015) 59–68

Contents lists available at ScienceDirect

Toxicology

journal homepage: www.elsevier.com/locate/toxicol

# Subacute nicotine co-exposure has no effect on 2,2′,3,5′,6-pentachlorobiphenyl disposition but alters hepatic cytochrome P450 expression in the male rat

Marianna Stamou[a,1], Eric Uwimana[b,1], Brenna M. Flannery[a], Izabela Kania-Korwel[b], Hans-Joachim Lehmler[b], Pamela J. Lein[a,*]

[a] Department of Molecular Biosciences, School of Veterinary Medicine, University of California, Davis, CA, USA
[b] Department of Occupational and Environmental Health, College of Public Health, The University of Iowa, Iowa City, IA, USA

ARTICLE INFO

*Article history:*
Received 11 June 2015
Received in revised form 30 September 2015
Accepted 6 October 2015
Available online 14 October 2015

*Keywords:*
Cytochrome P450 enzymes
CYP1A2
CYP2B1
CYP2B3
CYP3A2
Disposition
Atropselective
Nicotine
Polychlorinated biphenyls
Wistar rat

ABSTRACT

Polychlorinated biphenyls (PCBs) are metabolized by cytochrome P450 2B enzymes (CYP2B) and nicotine is reported to alter CYP2B activity in the brain and liver. To test the hypothesis that nicotine influences PCB disposition, 2,2′,3,5′,6-pentachlorobiphenyl (PCB 95) and its metabolites were quantified in tissues of adult male Wistar rats exposed to PCB 95 (6 mg/kg/d, p.o.) in the absence or presence of nicotine (1.0 mg/kg/d of the tartrate salt, s.c.) for 7 consecutive days. PCB 95 was enantioselectively metabolized to hydroxylated (OH-) PCB metabolites, resulting in a pronounced enrichment of $E_1$-PCB 95 in all tissues investigated. OH-PCBs were detected in blood and liver tissue, but were below the detection limit in adipose, brain and muscle tissues. Co-exposure to nicotine did not change PCB 95 disposition. CYP2B1 mRNA and CYP2B protein were not detected in brain tissues but were detected in liver. Co-exposure to nicotine and PCB 95 increased hepatic CYP2B1 mRNA but did not change CYP2B protein levels relative to vehicle control animals. However, hepatic CYP2B protein in animals co-exposed to PCB 95 and nicotine were reduced compared to animals that received only nicotine. Quantification of CYP2B3, CYP3A2 and CYP1A2 mRNA identified significant effects of nicotine and PCB 95 co-exposure on hepatic CYP3A2 and hippocampal CYP1A2 transcripts. Our findings suggest that nicotine co-exposure does not significantly influence PCB 95 disposition in the rat. However, these studies suggest a novel influence of PCB 95 and nicotine co-exposure on hepatic cytochrome P450 (P450) expression that may warrant further attention due to the increasing use of e-cigarettes and related products.



## 1. Introduction

Nicotine is a highly addictive component of cigarette smoke, e-cigarettes and other tobacco products (Yamin et al., 2010; Noel et al., 2011; Regan et al., 2013) that rapidly crosses the blood–brain barrier to upregulate cytochrome P450 enzymes (Anandatheerthavarada et al., 1993a; Miksys et al., 2000). CYP2B6 is upregulated in the brain of human smokers (Miksys et al., 2003), and nicotine has been reported to increase CYP2B expression in the brain of rats and non-human primates while either reducing or not changing hepatic CYP2B expression (Miksys et al., 2000; Lee et al., 2008). These effects of nicotine on CY2B expression in the brain have been linked to altered *in vivo* pharmacokinetics and pharmacodynamics of the neuroactive compound propofol (Khokhar and Tyndale, 2011).

Human CYP2B6 also metabolizes neurotoxic environmental contaminants including polychlorinated biphenyls (PCBs) (Ariyoshi et al., 1995; Warner et al., 2008), polybrominated diphenyl ethers (PBDEs) (Feo et al., 2012) and organophosphorus pesticides (Crane et al., 2012). CYP2B-mediated metabolism alters the neurotoxic potential of PCBs and PBDEs (Kim et al., 2011; Niknam et al., 2013), and is important in both bioactivation and detoxification of organophosphorus pesticides (Foxenberg et al., 2011). Collectively, these studies suggest that nicotine exposure may influence neurotoxicity by modulating CYP2B activity in the

*Abbreviations:* $C_t$, fractional amplification (cycle number at which fluorescence exceeds a user-defined threshold); d, day; b.w., body weight; DE, diatomaceous earth; EF, enantiomeric fraction; qPCR, quantitative (real-time) polymerase chain reaction; PCBs, polychlorinated biphenyls; P450, cytochrome P450.

* Corresponding author at: Department of Molecular Biosciences, UC Davis School of Veterinary Medicine, 1089 Veterinary Medicine Drive, Davis, CA 95616, USA. Fax: +1 530 752 7690.
*E-mail address:* pjlein@ucdavis.edu (P.J. Lein).

[1] These authors contributed equally to this manuscript.

http://dx.doi.org/10.1016/j.tox.2015.10.002
0300-483X/

brain or liver, thereby altering toxicant levels local to cellular targets.

Here we test the hypothesis that repeated nicotine co-exposure alters the disposition of PCB 95 and its metabolites. PCB 95 was chosen for these studies because it is linked to neurotoxic outcomes in humans and rats (Pessah et al., 2010) and it is metabolized by CYP2B1 in rats (Warner et al., 2008; Lu et al., 2013). Furthermore, PCB 95 is a chiral molecule that exists as two non-superimposable mirror images called enantiomers, and the CYP2B-mediated metabolism of PCB 95 is enantioselective (Lu et al., 2013; Kania-Korwel and Lehmler, 2015). Thus, monitoring the enantiomeric signatures of PCB 95 and its metabolites is expected to provide a sensitive readout for investigating changes in P450 enzyme activities in the brain.

We detected PCB 95 in all tissues investigated, including the cortex and cerebellum, and observed considerable enantiomeric enrichment of the first eluting PCB 95 atropisomer; however, co-exposure to nicotine did not alter PCB 95 disposition in the brain or liver. CYP2B1 mRNA and CYP2B protein were not detected in rat brain, and nicotine treatment had no significant effect on levels of CYP2B1, CYP2B3, CYP3A2 and CYP1A2 mRNA or CYP2B protein in the brain. In contrast, we observed a novel influence of PCB and nicotine co-exposure on the expression of hepatic CYP2B1 and CYP3A2 mRNA.

## 2. Material and methods

### 2.1. Chemicals

2,2′,3,5′,6-Pentachlorobiphenyl (PCB 95; 99.7% purity), 2,3,4′,5,6-pentachlorobiphenyl (PCB 117; 99% purity), 2,2′,3,4,4′,5,6,6′-octachlorobiphenyl (PCB 204; 99.9% purity) and 2′,3,3′,4,5,5′-hexachlorobiphenyl-4′-ol (4-159, >99.9% purity) were purchased from AccuStandard (New Haven, CT, USA). 3-Methoxy-2,2′,4,5′,6-pentachlorobiphenyl (3-103), 2,2′,3,5′,6-pentachlorobiphenyl-4-ol (4-95), 2,2′,3,5′,6-pentachlorobiphenyl-4′-ol (4′-95), 2,2′,3,5′,6-pentachlorobiphenyl-5-ol (5-95) and 4,5-dimethoxy-2,2′,3,5′,6-pentachlorobiphenyl (4,5-95) were synthesized at >95% purity as described previously (Kania-Korwel et al., 2008; Joshi et al., 2011). The respective chemical structures and abbreviations are shown in Fig. 1. (−)-Nicotine hydrogen tartrate salt (98% purity; CAS number 65-31-6) was purchased from Sigma–Aldrich (St. Louis, MO, USA). $^{1}H$ and $^{13}C$ NMR spectra confirmed that the nicotine hydrogen tartrate salt was highly pure (see Supplemental data, Figs. S1 and S2).

### 2.2. Animals and treatments

Animals were maintained in facilities fully accredited by the Association for Assessment and Accreditation of Laboratory Animal Care International, and all studies were carried out in accordance with the Guide for the Care and Use of Laboratory Animals as adopted and promulgated by the U.S. National Institutes of Health, and with regard for alleviation of pain and suffering under protocols approved by the UC Davis Institutional Animal Care and Use Committee. Adult male Wistar rats (50–55 days old; 209–270 g; Charles River Laboratories, Hollister, CA) were housed individually in standard plastic cages under controlled environmental conditions (22 ± 2 °C, 40–50% humidity) with a normal 12 h light/dark cycle. Food and water were provided *ad libitum*.

Animals were allowed to acclimate for 48 h after delivery to the UC Davis vivarium and then randomly divided into eight experimental groups with four animals per experimental group (Fig. 2): (i) nicotine in sterile saline (1 mg/kg/d, s.c.) for 7 d plus PCB 95 (6 mg/kg/d, p.o. in peanut butter) for days 1–6; (ii) an equal volume of vehicle (sterile saline, 0.3 ml/d, s.c.) for 7 d plus PCB 95 (6 mg/kg/d, p.o. in peanut butter) for days 1–6; (iii) nicotine in sterile saline (1 mg/kg/d, s.c.) for 7 d; or (iv) vehicle (sterile saline, 0.3 ml/d, s.c.) for 7 d. To assess transient effects of nicotine on CYP2B1 expression in the brain, a subset of rats were injected daily with: (v) nicotine (1 mg/kg/d, s.c.) for 1 d or (vi) 3 d; or (vii) an equal volume of vehicle (sterile saline, 0.3 ml/d, s.c.) for 1 d or (viii) 3 d (Fig. 2).

The dose and route of administration of nicotine was based on previous studies demonstrating that daily s.c. injection with 0.3 mg/kg nicotine free base for 7 consecutive days significantly increased CYP2B1 mRNA levels in the cortex of adult male Wistar rats compared to vehicle controls (Miksys et al., 2000). The tartrate salt of nicotine was administered at 1 mg/kg b.w. (2 μmol/kg b.w.), which translates to a dose of 325 μg/kg of nicotine as the free base (Matta et al., 2007). This dose results in blood nicotine levels in the rat comparable to levels in human smokers following 10 cigarettes (Le Houezec et al., 1993). The PCB 95 dose (6 mg/kg/d, which equals 18.4 μmol/kg/d) was based on our previous studies of PCB 95 enantiomeric disposition in the mouse brain (Kania-Korwel et al., 2012). The route of administration of PCB 95 was previously described (Kania-Korwel et al., 2012), and rats consumed the peanut butter mix within minutes.

Animals were euthanized by carbon dioxide inhalation 4 h after the last nicotine injection (approximately 28 h after the last

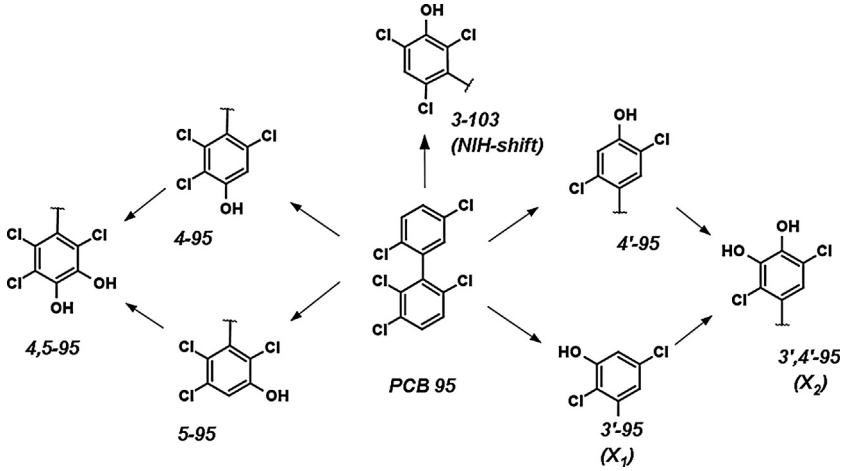


**Fig. 1.** Simplified scheme of PCB 95 biotransformation showing metabolites unambiguously identified with authentic standards, as well as two unknown metabolites tentatively identified as 3′-95 ($X_1$) and 3′,4′-95 ($X_2$).

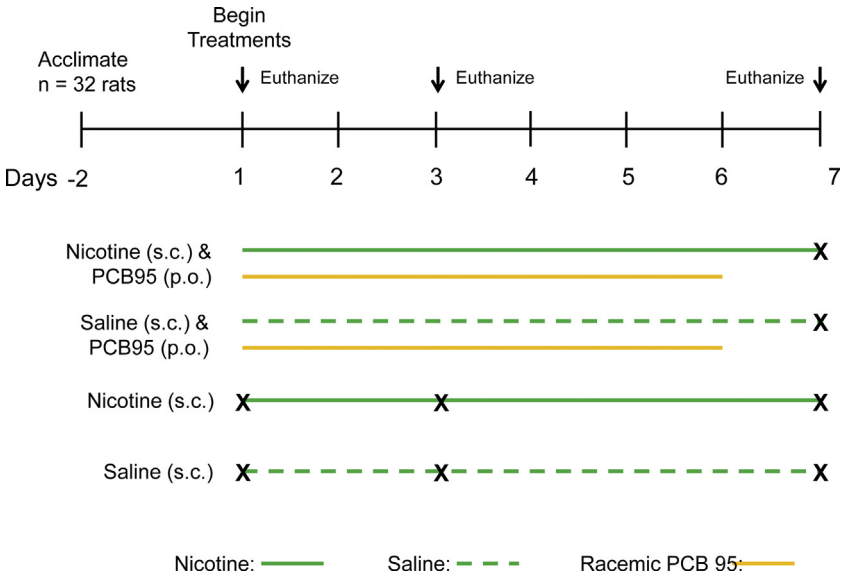


**Fig. 2.** Schematic illustrating the experimental design. Animals were randomly divided into eight experimental groups ($n = 4$ animals per experimental group) and dosed with (i) nicotine in saline for 7 d plus PCB 95 for days 1–6; (ii) saline for 7 d plus PCB 95 for days 1–6; (iii) nicotine in saline for 7 d; (iv) saline for 7 d; (v) nicotine in saline for 3 d; (vi) nicotine in saline for 1 d; (vii) saline for 3 d; or (viii) saline for 1 d. Nicotine was administered as the tartrate salt at 1 mg/kg/d, s.c.; PCB was administered at 6 mg/kg/d, p.o.

PCB 95 administration). Blood, muscle (*biceps femoris*), adipose, liver, and brains were immediately collected and brains were microdissected on ice to isolate the cortex, hippocampus and cerebellum. All tissues used for analysis of tissue PCB levels were wrapped in aluminum foil, snap-frozen in liquid nitrogen and stored at −80 °C until analyzed. Tissues used for qPCR and western blot analyses were stored overnight in RNAlater (Life Technologies). The following morning, samples were removed from RNAlater and stored at −80 °C until further processed.

### 2.3. PCB and OH-PCB tissue extraction, clean-up and analysis

Tissue samples were extracted as described previously (Kania-Korwel et al., 2012). Briefly, cortex (0.15–0.31 g), cerebellum (0.098–0.190 g), liver (0.26–0.46 g), blood (0.65–1.28 g), muscle (0.19–0.46 g), and adipose (0.040–0.080 g) samples were homogenized with pre-extracted diatomaceous earth (DE) (2 g) and placed in 33 ml size extraction cells over pre-extracted Florisil® (12 g). Blood aliquots were evenly distributed on top of extraction cells containing pre-extracted Florisil and pre-extracted DE. Each batch of samples was accompanied by a method blank (DE and Florisil only, no tissue) and matrix blanks (tissue from non-PCB exposed animal). Surrogate recovery standards, PCB 117 (50 ng) and 4–159 (68.5 ng), were added to each cell. The samples were extracted using a pressurized solvent extraction system (ASE 200, Dionex®, Sunnyvale, CA, USA) with hexane: dichloromethane: methanol (48:43:9, v/v) as solvent at 100 °C, 1500 psi (10 MPa) with preheat equilibration of 6 min, 35% cell flush volume, and 1 static cycle of 5 min. The extracts were concentrated, derivatized with diazomethane and subjected to a sulfur cleanup step (Kania-Korwel et al., 2007, 2008).

The final organic extract was analyzed using an Agilent 7870A gas chromatograph equipped with a $^{63}$Ni micro-electron capture detector (GC-ECD) and a SPB 1 column (60 m, 0.25 mm inner diameter, 0.25 μm film thickness; Supelco, St. Louis, MO, USA) (Kania-Korwel et al., 2012). The injector was operated in splitless mode at a temperature of 280 °C, with the detector temperature at 300 °C. The temperature program started at 50 °C for 1 min, then 30 °C/min to 200 °C, 1 °C/min to 250 °C, and 10 °C/min to 280 °C. Concentrations of PCB 95 and its hydroxylated metabolites (as methylated derivatives) were determined using PCB 204 as the internal standard. The overall recoveries of PCB 117 and 4–159 were 104 ± 39% and 65 ± 20%, respectively. Limits of detection for the quantification of PCB 95 and its metabolites in tissues are summarized in Table S1, Supplemental data. The presence of several hydroxylated PCB 95 metabolites identified in the GC-ECD analysis (Fig. S3) was confirmed by gas chromatography–mass spectrometry (GC–MS) analysis, as shown in Fig. S4.

Enantioselective analyses of PCB 95 were performed on an Agilent 7890 gas chromatograph equipped with a $^{63}$Ni μ-ECD and a Chirasil-Dex column (2,3,6-tri-*O*-methyl-β-cyclodextrin; 30 m, 250 μm inner diameter, 0.12 μm film thickness; Agilent, Santa Clara, CA, USA) (Kania-Korwel et al., 2012). The following temperature program was used: initial temperature was held at 90 °C for 1 min, then increased at 30 °C/min to 160 °C, hold for 20 min, 1 °C/min to 170 °C, hold for 7 min, 1 °C/min to 190 °C, hold for 20 min, 10 °C/min to 200 °C, hold for 20 min. Since the elution order of the PCB95 atropisomers is unknown, the enantiomeric fractions (EF) were calculated as $EF = A1/(A1 + A2)$ where $A1$ and $A2$ are the peak area of the first and the second eluting PCB 95 atropisomers (Kania-Korwel et al., 2012). The EF of racemic PCB 95 was 0.498 ± 0.007 ($n = 7$), with a resolution of the PCB 95 atropisomers of 0.8 ± 0.1 on the Chirasil-Dex column. Enantioselective analyses of PCB 95 in cerebellum and of OH-PCBs in all tissues investigated were not possible due to their low levels in the tissue extracts.

### 2.4. Preparation of microsomes from liver and cortex

Microsomes were prepared as previously described with minor modifications (Khokhar et al., 2010). Briefly, frozen samples of liver and cortex were thawed and homogenized in buffer containing 0.1 M Tris (pH 7.4), 0.32 M sucrose, 1% EDTA and 1% dithiothreitol, using a Polytron PT 1200E tissue homogenizer (Kinematica, Bohemia, NY). The homogenate was centrifuged twice at 9000 × *g* for 5 min at 4 °C. The supernatant was then ultracentrifuged at 110,000 × *g* for 90 min at 4 °C. The resulting pellet was suspended in 0.1 M Tris buffer (pH 7.4) containing 1.15% potassium chloride, 20% glycerol, 1% EDTA and 1% dithiothreitol and stored at −80 °C until further use. Microsomal protein concentrations were determined using the Pierce BCA Protein Assay Kit (Thermo Scientific, Waltham, MA).

### 2.5. Western blot analysis of CYP2B protein

Total protein from liver and cortical microsomes (30 μg microsomal protein per lane) was separated by SDS PAGE using Bolt Bis–Tris Plus Gels (Life Technologies, Carlsbad, CA), transferred onto PVDF membranes (iBlot Transfer Stacks, Life Technologies) using the iBlot 2 dry transfer system (Life Technologies) and immunoblotted using the iBind Western System (Life Technologies). Blots were probed with 2 different CYP2B antibodies: (i) a commercially available mouse monoclonal antibody that recognizes CYP2B1/2 (10R-C154A, Batch number 91895 DM, Fitzgerald Industries International, Acton, MA) and was previously used in immunoprecipitation experiments to assess CYP2B1 activity in adult male Wistar rat brains (Khokhar et al., 2010; Khokhar and Tyndale, 2011); and (ii) a rabbit polyclonal anti-CYP2B IgG antibody (generously provided by Stelvio Bandiera, University of British Columbia) previously demonstrated to react with rat liver CYP2B1, CYP2B2 and a third non-inducible enzyme of the CYP2B family but not with any other rat P450 proteins (Panesar et al., 1996). All samples were also probed with a rabbit monoclonal anti-GAPDH (2118, Lot number 8, Signaling Systems, Danvers, MA) (Siemens et al., 2011) as a loading control. The CYP2B1/2 Ab from Fitzgerald Industries was used at 1:20 dilution; the CYP2B Ab from Dr. Bandiera, at 20 μg/ml (1:130 dilution); and the anti-GAPDH at 1:200 dilution. Antibody-antigen complexes were detected using IRDye800-conjugated goat anti-rabbit IgG (611-132-122, Lot number 23641, Rockland, Gilbertsville, PA, diluted 1:2000), to detect the rabbit anti-GAPDH and the rabbit anti-CYP2B1, and IRDye700DX-conjugated goat anti-mouse IgG (610-130-121, Lot number 13508, Rockland, diluted 1:2000) to detect the mouse anti-CYP2B1. Membranes were scanned using the Odyssey Infrared Imaging System (LI-COR) to identify immunopositive bands. Proteins were identified based on size (approximately 56 kDa for CYP2B and 37 kDa for GAPDH). Each sample was analyzed in three independent experiments, randomizing the order of sample loading each time. Samples containing only loading buffer were used as negative controls. Microsomal protein (0.13 μg/lane) from the livers of phenobarbital-induced adult male Sprague Dawley rats (Wu et al., 2011); and cDNA-expressed CYP2B1 (Supersomes; 456510, Corning, Woburn, MA; 3 μg/lane) were used as positive controls. Densitometric analysis of immunoblots was performed using Image Studio Lite 4.0 software (Licor Biotechnology, Lincoln, NE). Densitometric data for CYP2B immunopositive bands were normalized to GAPDH immunopositive bands from the same sample.

### 2.6. Quantitative polymerase chain reaction analyses

Total RNA extraction, cDNA synthesis and quantitative polymerase chain reaction (qPCR) were performed at the Real-Time PCR Research and Diagnostics Core Facility at UC Davis. Analysis of the results and quantification of gene transcript levels was performed using SDS 2.4.1 (Applied Biosystems, Carlsbad, CA) and REST 2009 software (Qiagen, Valencia, CA). Transcripts were quantified for the target genes CYP2B1, CYP2B3, CYP3A2 and CYP1A2; transcripts were also quantified for three reference genes: phosphoglycerate kinase 1 (Pgk1), peptidylpropyl isomerase A (Ppia) and hypoxanthine-guanine phosphoribosyl transferase (Hprt). The primer and probe sequences for each of these transcripts are listed in Table S2 of Supplemental data. The specificity of our primer set for CYP2B1 (Stamou et al., 2014) has been confirmed using the BLASTN function on the NCBI website (http://www.ncbi.nlm.nih.gov/tools/primer-blast), and is not predicted to amplify CYP2B2 or any other P450 of the *Rattus Norvegicus* species.

The expression of target genes were normalized either against Pgk1 expression alone or against the geometric mean of the expression of Pgk1, Ppia and Hprt within the same sample, and the relative expression ratios between treated and vehicle control animals were calculated by the Pfaffl method (Pfaffl, 2001), using the REST 2009 software as previously described (Stamou et al., 2014). A more detailed description of these methods is provided in the Supplemental data.

### 2.7. Statistical analysis

Treatment-related differences in the levels of the PCB 95 parent compound and hydroxylated metabolites were analyzed using Student's *t*-test. EF values were compared between the experimental groups and against the racemic standard using Student's *t*-test. Student's *t*-test was performed with adjustment for multiple comparisons, with $p < 0.05$ considered significant. Statistical analysis of the qPCR data was performed using the built-in randomization techniques of REST 2009 software (Stamou et al., 2014) as described in the Supplemental data. Densitometric data were analyzed by one-way ANOVA with Tukey's *post hoc* test using Graphpad Prism (v. 5.01, La Jolla, CA).

## 3. Results

### 3.1. Effect of nicotine co-exposure on the disposition of PCB 95

Adult male Wistar rats were co-exposed to nicotine and PCB 95 (experimental groups (i) and (ii); Fig. 2), and levels of the PCB 95 parent compound (Fig. 3) and its hydroxylated metabolites (Fig. 4) were quantified in cortex, cerebellum, adipose, blood, liver and muscle. The small size of the hippocampus precluded measurements of PCB 95 or its metabolites in this brain region. The parent PCB was readily detected in the cortex and cerebellum (Fig. 3A). Co-exposure to nicotine for 7 d had no effect on the levels of the parent compound in any tissue investigated (Fig. 3A). In both experimental groups, the levels of PCB 95 were significantly higher in adipose than in the other tissues investigated and decreased in the rank order adipose > liver > cerebellum∼cortex∼skeletal muscle > blood (Fig. 3A and Table S3 of the Supplemental data). These observations are consistent with previous reports indicating that the highest levels of chiral PCB congeners, including PCB 95, are found in the adipose (Birnbaum, 1983; Kania-Korwel et al., 2012), which is the major storage site for lipophilic compounds.

No hydroxylated PCB 95 metabolites were detected in the cortex, cerebellum or skeletal muscle of animals exposed to PCB 95 in the absence or presence of nicotine. In adipose tissue, only 5–95 was detected as a minor metabolite in both experimental groups (data not shown). However, consistent with previous findings in mice (Kania-Korwel et al., 2012), several OH-PCB metabolites were detected in the blood (Fig. 4A) and liver (Fig. 4B) of both experimental groups, including 3–103 (1,2-shift product), 4–95, 4′–95, 5–95 and 4,5–95. In both groups, 4,5–95 was a major metabolite in blood (Fig. 4A), while 4′–95, 5–95 and 4,5–95 were the predominant metabolites in the liver (Fig. 4B). In addition to the OH-PCB metabolites shown in Fig. 4, two unknown metabolites were detected in the liver in both experimental groups and in the pooled blood sample from both experimental groups (Figs. S3 and S4 of the Supplemental data). Based on their molecular weight and retention time, these metabolites are likely 3′–95 and 3′,4′–95; however, neither metabolite could be unambiguously identified because authentic standards were not available. Importantly, no statistically significant differences were observed in the levels of any of the identified metabolites in blood or liver of animals co-exposed to nicotine and PCB 95 *versus* animals exposed to PCB 95 alone (Fig. 4A and B).

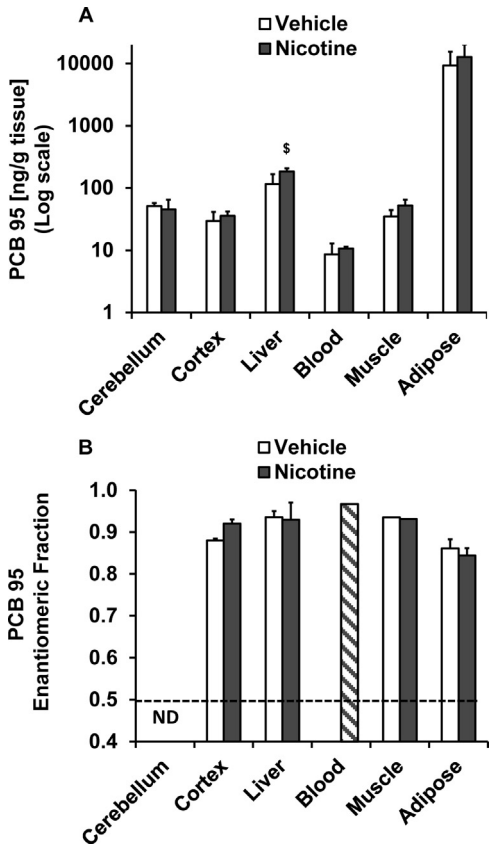


**Fig. 3.** Co-exposure to nicotine does not alter the levels and enantiomeric fractions of PCB 95 in the male rat brain or peripheral tissues. (A) Levels of the parent compound PCB 95 in the cortex and cerebellum of rats co-exposed to nicotine and PCB 95 were not significantly different than in rats exposed to vehicle (saline) and PCB 95. Similarly, nicotine co-treatment had no effect on PCB 95 levels in liver, blood, adipose or muscle (Student's *t*-test; $p < 0.05$; $n = 4$ animals per experimental group). Specific tissue concentrations are provided in Table S4 of the Supplemental data. (B) Nicotine co-exposure did not significantly modify PCB 95 atropisomer distribution, expressed as the enantiomeric fraction (EF) of the first-eluting atropisomer of PCB 95 on a Chirasil-Dex column relative to the two isomers combined (Student's *t*-test; $p < 0.05$; $n = 4$ animals per experimental group, unless otherwise noted). The first-eluting atropisomer ($E_1$-PCB 95) displayed a pronounced enrichment in both experimental groups across all tissues investigated. Because of the low PCB 95 levels in blood and muscle, extracts from all blood samples ($n = 8$) and all muscle samples within each experimental group ($n = 4$ animals per experimental group) were pooled to allow EF determination in a single sample. Otherwise, all data represent the mean ± standard deviation. The dashed line corresponds to the EF of the racemic PCB 95 standard. All EF values were significantly different from the racemic standard (Student's *t*-test; $p < 0.05$). ND not detected. $^{\$}p = 0.052$. Bar with downward diagonals: EF of all blood samples ($n = 8$) pooled into a single sample. Data are from experimental groups (i) and (ii) as described in Section 2.2 and illustrated in Fig. 2.

### 3.2. Effect of nicotine co-exposure on the enantioselective enrichment of PCB 95

In mice, PCB 95 and its metabolites exhibit enantiomeric enrichment in the brain that is either a result of enantioselective hepatic metabolism by CYP2B1 enzymes (Kania-Korwel et al., 2012; Lu et al., 2013) or may be mediated by localized metabolism in the brain (Dutheil et al., 2010; Miksys and Tyndale, 2013). Because changes in the enantiomeric enrichment of PCB 95 are likely sensitive to altered CYP2B expression (Lehmler et al., 2010), we evaluated the enantiomeric enrichment of PCB 95 and its metabolites in the brain and peripheral tissues from both experimental groups dosed with PCB 95 (Fig. 2). Enantioselective analysis for the PCB 95 parent compound on a Chirasil-Dex column revealed predominant enrichment of the first eluting atropisomer of PCB 95 ($E_1$-PCB 95; $E_1$ and $E_2$ denote the elution order of the enantiomers in the enantioselective analysis), with EF values ranging from 0.84 to 0.97 (Fig. 3B; Table S5). Enrichment of $E_1$-PCB 95 was confirmed by spiking samples with a low amount of PCB 95 racemic standard and reanalyzing the samples. In both experimental groups, tissue EF values for PCB 95 followed the rank order: blood (sample pooled across experimental groups) > liver∼muscle (samples pooled within experimental groups) > cortex > adipose. There were no significant differences in the EF values of PCB 95 between the nicotine + PCB 95 *versus* saline + PCB 95 treatment groups (*e.g.*, experimental groups (i) and (ii)).

### 3.3. Effect of nicotine treatment on CYP2B protein levels in rat brain or liver

To determine whether nicotine altered the expression of CYP2B protein in the brain or liver at the dose investigated, western blotting was used to quantify CYP2B proteins in microsomes isolated from the cortex and liver of animals treated with saline, nicotine, saline plus PCB 95, or nicotine plus PCB 95 (experimental groups (i)–(iv), see Fig. 2). Proteins at the expected molecular weight for CYP2B1/2 (56 kDa) were not detected in any cortex or liver microsomes when blots were probed with a monoclonal antibody obtained from the same source as one previously used to quantify CYP2B1 protein in the adult male Wistar brain by immunoprecipitation (Khokhar et al., 2010; Khokhar and Tyndale, 2011) (data not shown). This antibody also did not react with liver microsomes from phenobarbital-induced rats or with recombinant CYP2B1 (data not shown). Microsomal preparations were then probed using a different antibody previously shown to selectively recognize CYP2B1, CYP2B2 and an unidentified non phenobarbital-inducible CYP2B enzyme (Panesar et al., 1996). This second antibody recognized recombinant rat CYP2B1 and reacted robustly with liver microsomes from phenobarbital-induced rats (Fig. 5). This antibody also cross-reacted with proteins at ∼56 kDa in liver but not cortical microsomes from all four experimental groups (Fig. 5A–C). Densitometric analyses of CYP2B immunoreactive bands indicated that neither nicotine nor PCB 95 alone changed hepatic CYP2B levels relative to vehicle controls. However, co-exposure to nicotine and PCB 95 significantly decreased levels of CYP2B protein in liver microsomes relative to nicotine exposure alone (Fig. 5D).

### 3.4. Effect of co-exposure to nicotine and PCB 95 on CYP2B1 mRNA expression

CYP2B1 transcripts were quantified using qPCR to further investigate whether nicotine upregulates CYP2B1 in the brain or liver using two different primer/probe sets: (i) a primer/probe set previously designed and validated in our laboratory (Stamou et al., 2014), which was confirmed to be specific for CYP2B1 and predicted to not amplify CYP2B2 or any other P450 of the *R. Norvegicus* species (see Section 2.6); and (ii) a set consisting of a primer pair previously used to show nicotine-induced CYP2B1 expression in the brain (Miksys et al., 2000), which when blasted against the *R. Norvegicus* genome, identified CYP2B3 as a potential non-intended target. The second primer set was combined with a probe designed in-house (Table S2 of the Supplemental data).

CYP2B1 mRNA was not detected by either CYP2B1 primer/probe set in the cortex, hippocampus or cerebellum of any experimental group (Tables 1 and 2), suggesting that exposure to PCB 95 or nicotine alone or in combination did not induce CYP2B1 mRNA expression in the brain. In contrast, CYP2B1 mRNA was detected in the liver of all animals across all experimental groups (Tables 1 and 2). Exposure to either nicotine or PCB 95 alone did not significantly change hepatic CYP2B1 transcript levels relative to vehicle controls

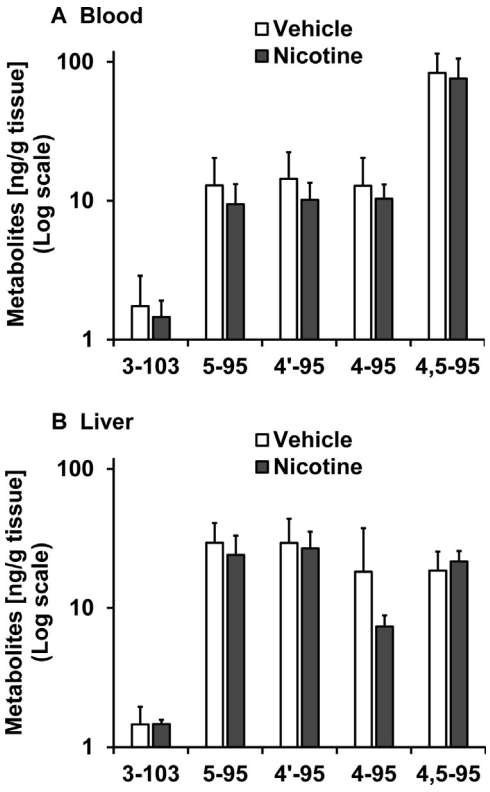


**Fig. 4.** Levels of OH-PCB 95 metabolites in (A) blood and (B) liver are not significantly altered by nicotine co-exposure in male Wistar rats. Data are from experimental groups (i) and (ii) as described in Section 2.2 and illustrated in Fig. 2. Data are presented as the mean ± standard deviation ($n = 4$ animals per experimental group). No statistically significant differences between experimental groups were identified using Student's $t$-test at $p < 0.05$. Specific tissue levels of OH-PCB 95 metabolites are reported in Table S4.

(Table 2); however, co-exposure to nicotine and PCB 95 significantly increased hepatic CYP2B1 mRNA levels (2.8-fold; $p = 0.04$; $n = 4$ animals per experimental group) relative to vehicle controls, but not relative to animals exposed to either nicotine or PCB 95 alone (Table 2).

### 3.5. Effect of co-exposure to nicotine and PCB 95 on transcript levels of other P450 enzymes in rat brain and liver

To further characterize the effects of nicotine and PCB 95 on P450 mRNA expression in the brain and liver, transcript levels of additional P450 enzymes were quantified including: (i) CYP3A2 and CYP1A2, both of which have previously been implicated in the metabolism of persistent organic pollutants, including PCBs (Hrycay and Bandiera, 2003); and (ii) CYP2B3, which is highly homologous to CYP2B1. Both CYP2B1 and CYP2B3 are homologous (86% and 78%, respectively) to human CYP2B6. CYP2B6 has been reported to be increased in the brain of smokers in a pilot study (Miksys et al., 2003) and is thought to be involved in PCB metabolism in humans (Ariyoshi et al., 1995; Warner et al., 2008).

CYP1A2 mRNA was detected in cortex, hippocampus and cerebellum across all eight experimental groups (Tables 1 and 2), whereas CYP2B3 and CYP3A2 transcripts were detected only in cerebellum. Exposure to nicotine alone or in combination with PCB 95 did not alter P450 mRNA expression profiles in cortex or cerebellum (Tables 1 and 2). In the hippocampus, treatment with nicotine alone for 3, but not 1 or 7 consecutive days, downregulated CYP1A2 mRNA relative to vehicle control (0.54-fold decrease, $p = 0.013$, 95% confidence interval = 0.331–0.779; Table 1). Neither nicotine nor PCB 95, alone or in combination, altered hippocampal expression of CYP2B3 or CYP3A2 mRNA (Tables 1 and 2).

In the liver, CYP1A2, CYP2B3 and CYP3A2 mRNA was detected across all experimental groups (Tables 1 and 2). CYP2B3 and CYP1A2 mRNA were unchanged by exposure to nicotine or PCB 95, alone or in combination. However, co-exposure to nicotine and P CB 95 upregulated CYP3A2 transcripts relative to all other experimental conditions (Table 2): 3.54-fold increase compared to nicotine only ($p = 0.008$, 95% CI: 1.790–6.441); 2.38-fold increase compared to vehicle control ($p = 0.006$, 95% CI: 1.187–4.911); and 1.87-fold increase compared to PCB 95 only ($p = 0.04$, 95% CI: 0.893–3.508). Exposure to PCB 95 alone did not change hepatic CYP3A2 mRNA relative to vehicle control.

## 4. Discussion

The goal of this study was to determine whether nicotine co-exposure modifies the enantioselective disposition of a neurotoxic PCB congener in the brain via changes in brain and/or hepatic CYP2B levels. PCB 95 was detected in all tissues investigated, including the brain (cortex and cerebellum). The hydroxylated metabolites of PCB 95 were detected in the liver and blood, but not the brain of animals exposed to PCB 95, which is in agreement with previous findings in mice (Kania-Korwel et al., 2012). Nicotine co-exposure did not change levels of either the PCB 95 parent compound or its metabolites in any tissue investigated. We observed significant enantiomeric enrichment of the $E_1$-PCB 95 enantiomer in the cortex. While enantiomeric enrichment of PCB 95 has also been observed in mice, in contrast to rat, $E_2$-PCB 95 is enriched in the mouse brain (Kania-Korwel et al., 2012). Co-exposure to nicotine had no significant effect on the enantiomeric enrichment of PCB 95 in the cortex or in peripheral tissues. Because the structurally related 2,2′,3,3′,6,6′-hexachlorobiphenyl (PCB 136) atropselectively affects neuronal connectivity (Pessah et al., 2009; Yang et al., 2014), further studies are needed to assess the toxicological relevance of the highly species-dependent atropisomeric enrichment in rats *versus* mice.

The lack of effect of nicotine on the disposition of PCB 95 in the adult male rat brain most likely is due to the fact that CYP2B expression was not induced by nicotine treatment in any experimental group in our study. While our finding is consistent with a previous report that a 20 day exposure to tobacco smoke did not upregulate CYP2B1/2 in adult female Wistar rats (Czekaj et al., 2000), it is in contrast to previous studies of adult male Wistar rats (Miksys et al., 2000; Khokhar et al., 2010). One potential explanation for the discrepancy between our observations and these latter studies is the dose of nicotine used. While one of these latter studies (Miksys et al., 2000) did show increased CYP2B expression in the brain following 7 d of repeated injections of nicotine base at 300 μg/kg/d, these changes were primarily limited to the brain stem and olfactory cortex with no change in CYP2B mRNA in other brain regions and only modest (0.76-fold) increase in CYP2B protein in the frontal cortex. Significant increases in CYP2B mRNA and proteins levels in the frontal cortex, hippocampus and cerebellum were only observed in the brains of animals repeatedly injected with nicotine base at 1.0 mg/kg/d, which is approximately 3 times the dose we used (325 μg/kg/d, expressed as the free base).

Another key difference between our observations and the studies reported by the group that has demonstrated nicotine induction of brain CYP2B1 is that we did not detect constitutive expression of CYP2B1 mRNA in cortex, cerebellum and hippocampus or CYP2B protein in the cortex of adult male Wistar rats. While these findings agree with our previous observation that CYP2B1 mRNA is not detected in the adult Sprague Dawley rat

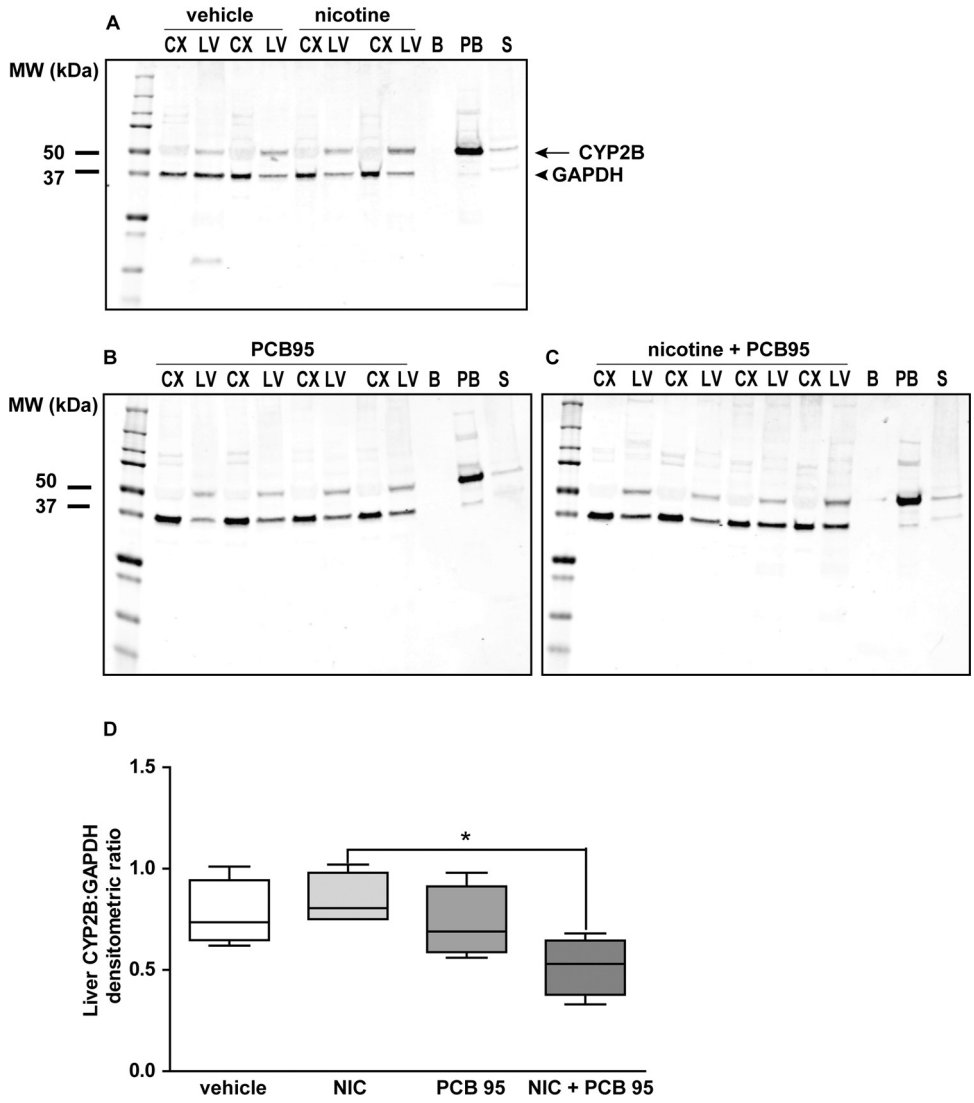


**Fig. 5.** Effect of nicotine and/or PCB 95 exposure on liver and brain CYP2B protein levels. Total protein of microsomes isolated from the liver and the cortex of rats treated with saline, nicotine, saline plus PCB 95, or nicotine plus PCB 95 (experimental groups (i)–(iv) as described in Section 2.2 and illustrated in Fig. 2) were separated by SDS gel electrophoresis and probed with a polyclonal antibody against CYP2B. Representative blots demonstrating detection of CYP2B (arrow) in liver (LV) but not cortical (CX) microsomes from (A) vehicle or nicotine-treated animals; (B) PCB 95-exposed animals; and (C) animals co-exposed to nicotine and PCB 95. GAPDH (arrowhead) was probed as a loading control. (D) Densitometric analyses of liver CYP2B protein normalized to GAPDH as a percentage of vehicle controls. Data are presented as box plots in which the horizontal line in each box represents the median, the boundary of the box represents the 25th–75th percentiles and the whiskers represent 1st–99th percentiles ($n = 4$ animals per experimental group). The CYP2B1/GAPDH densitometric ratio was significantly lower in the liver samples of animals co-exposed to PCB 95 and nicotine compared to animals exposed to nicotine alone (one-way ANOVA with Tukey *post hoc* test; $^*p < 0.05$). B, loading buffer control; PB, liver microsomes from an adult male rat treated with phenobarbital; S, supersomes (recombinant rat CYP2B1).

**Table 1**
Nicotine does not cause widespread changes in P450 mRNA levels in the brain or liver of adult male rats after 1 or 3 d of daily injections.[a]

| | Cortex | | Hippocampus | | Cerebellum | | Liver | |
|---|---|---|---|---|---|---|---|---|
| | 1 d | 3 d | 1 d | 3 d | 1 d | 3 d | 1 d | 3 d |
| CYP2B1 | ~ | ~ | ~ | ~ | ~ | ~ | 0.89 | 0.77 |
| CYP2B3 | ~ | ~ | ~ | ~ | 0.63 | 0.81 | 0.74 | 0.79 |
| CYP3A2 | ~ | ~ | ~ | ~ | 1.00 | 0.95 | 0.75 | 1.32 |
| CYP1A2 | 1.92 | 0.42 | 0.96 | ↓**0.54**[b] | 0.97 | 0.91 | 0.93 | 1.50 |

~, indicates mRNA was not detected.

[a] Adult male rats were injected with nicotine (1 mg/kg/d, s.c.) or an equal volume (0.3 ml) of vehicle (sterile saline) for 1 or 3 d (experimental groups (v)–(viii) in Fig. 2). The fold change in mRNA expression in tissues from nicotine-treated animals relative to vehicle controls was calculated using the REST2009 software (Qiagen), which incorporates $C_t$ and efficiency values determined by qPCR analysis (Stamou et al., 2014).

[b] ↓ indicates significant downregulation of gene expression ($p < 0.05$).

brain, even following treatment with the classic P450 inducers phenobarbital or dexamethasone at levels that induced hepatic P450 expression (Stamou et al., 2014), and they are consistent with a previous study of CYP2B expression in the brain of adult female Wistar rats (Czekaj et al., 2000), they are in contrast to studies that reported constitutive expression of CYP2B1 in the male rat brain (Miksys et al., 2000; Khokhar et al., 2010). Differences in the animals' environment, including housing, husbandry and diet, may account for differences in the constitutive levels of CYP2B1 in the brain between studies (Ronis et al., 1999; Kozul et al., 2008), which in turn may determine the response to nicotine.

An alternate explanation is that nicotine and/or PCB 95 altered the expression of P450 enzymes other than CYP2B1/2 and those changes offset the effect of nicotine on CYP2B1-mediated PCB 95 metabolism and/or changed the metabolism of nicotine itself. The latter possibility is suggested by evidence that PCBs can be metabolized by multiple P450s (Hrycay and Bandiera, 2003;

**Table 2**
Fold-change in P450 mRNA levels in adult male rats exposed to vehicle (saline), 1 mg/kg nicotine (s.c. once daily, days 1–7) or 6 mg/kg PCB95 (p.o. in peanut butter once daily, days 1–6) alone or in combination.[a]

| | Nicotine vs. vehicle | PCB 95 vs. vehicle | Nicotine + PCB 95 vs. vehicle | Nicotine + PCB 95 vs. nicotine | Nicotine + PCB 95 vs. PCB 95 |
|---|---|---|---|---|---|
| Cortex | | | | | |
| CYP2B1 | ~ | ~ | ~ | ~ | ~ |
| CYP2B3 | ~ | ~ | ~ | ~ | ~ |
| CYP3A2 | ~ | ~ | ~ | ~ | ~ |
| CYP1A2 | 6.74 | 0.95 | 2.16 | 0.32 | 2.28 |
| Hippocampus | | | | | |
| CYP2B1 | ~ | ~ | ~ | ~ | ~ |
| CYP2B3 | ~ | ~ | ~ | ~ | ~ |
| CYP3A2 | 1.64 | ~ | ~ | ~ | ~ |
| CYP1A2 | 0.49 | 0.18 | 0.19 | 0.38 | 1.11 |
| Cerebellum | | | | | |
| CYP2B1 | ~ | ~ | ~ | ~ | ~ |
| CYP2B3 | 0.57 | 0.29 | 0.32 | 0.49 | 1.10 |
| CYP3A2 | 1.05 | 0.59 | 0.90 | 0.86 | 1.53 |
| CYP1A2 | 1.15 | 1.98 | 2.11 | 1.84 | 1.06 |
| Liver | | | | | |
| CYP2B1 | 0.71 | 2.08 | ↑**2.81**[b] | 3.96 | 1.35 |
| CYP2B3 | 0.79 | 0.90 | 0.95 | 1.20 | 1.05 |
| CYP3A2 | 0.67 | 1.27 | ↑**2.38**[b] | ↑**3.54**[b] | ↑**1.87**[b] |
| CYP1A2 | 0.80 | 1.31 | 1.62 | 2.02 | 1.23 |

~, indicates mRNA was not detected.
[a] Corresponds to experimental groups (i)–(iv) in Fig. 2.
[b] Indicates statistically significant change (↑: upregulation/ ↓: downregulation) of gene expression ($p < 0.05$). The relative expression (shown in bold) was calculated using the REST2009 software (Qiagen), which incorporates $C_t$ and efficiency values determined by qPCR analysis (Stamou et al., 2014).

Warner et al., 2008; Kania-Korwel et al., 2012; Wu et al., 2013), and that both nicotine and PCB 95 can influence their own toxicokinetics by regulating the levels of P450 enzymes that metabolize them (Dannan et al., 1983; Miksys et al., 2000; Twaroski et al., 2001; Gahrs et al., 2013). However, in the present study, exposure to nicotine or PCB 95 alone or in combination did not cause widespread changes in the transcriptional profile of CYP1A2, CYP2B3 or CYP3A2 in the brain regions examined, in agreement with the lack of effect of classic P450 inducers on region-selective P450 expression of these transcripts in the rat brain (Stamou et al., 2014). The one exception to this generalization was that exposure to nicotine for 3 d, but not 1 or 7 d, downregulated hippocampal CYP1A2 expression. Evidence for CY1A2 transcriptional regulation by nicotine in liver and/or brain has been shown in rodents (Anandatheerthavarada et al., 1993b; Price et al., 2004), although in humans, nicotine has been reported to have no effect on CYP1A2 activity (Hukkanen et al., 2011). CYP1A2 has been implicated in PCB metabolism (Fitzgerald et al., 2005; Zhou et al., 2010; Curran et al., 2011); however, whether its transient downregulation in the hippocampus is functionally relevant to PCB neurotoxicity has yet to be determined.

Co-exposure to nicotine and PCB 95 significantly increased CYP3A2 and CYP2B1 mRNA in the liver. The increase in hepatic CYP2B1 mRNA was accompanied by a significant decrease in CYP2B protein in the liver. Discrepancies between CYP expression at the mRNA *versus* the protein level have been widely documented [reviewed by Collins et al. (2012)], and in a recent study of puromycin amino-nucleoside-induced cytotoxicity in glomerular epithelial cells, increased CYP2B1 mRNA was observed as a consequence of decreased CYP2B1 protein (Tian et al., 2010), suggesting the possibility that transcript levels are upregulated as a compensatory response to decreased protein levels. Collectively, these data support previous studies suggesting that transcriptional regulation of P450s in the brain is distinct from that in the liver (Meyer et al., 2007; Stamou et al., 2014). Furthermore, these data suggest that nicotine and PCB 95 interact to alter P450 expression in the liver but not in the brain. However, these changes in hepatic CYP2B1 expression are likely transient (Lee et al., 2008) and, therefore, not sufficient to significantly alter PCB 95 disposition at the dose used in our study.

## 5. Conclusions

Our study is the first to demonstrate that PCB 95 is enantioselectively metabolized to potentially neurotoxic OH-PCBs (Niknam et al., 2013) in the male rat, with a pronounced enrichment of $E_1$-PCB 95. However, in contrast to previous studies indicating that nicotine alters the kinetics and dynamics of neuroactive compounds metabolized by P450 enzymes, specifically chlorpyrifos (Lee et al., 2008) and propofol (Khokhar and Tyndale, 2011), nicotine did not significantly alter the disposition or enantiomeric enrichment of PCB 95 in the brain or peripheral tissues of adult male rats in our study. This can be explained in large part by our observations that CYP2B1/2 protein is not expressed in the brain of male rats and nicotine treatment alone does not significantly alter the expression of CYP2B1/2 and other P450 enzymes in the brain or liver. Although our data strongly suggest that PCB 95 disposition is not affected by exposure to nicotine, the P450 gene expression changes observed in animals co-exposed to nicotine and PCB 95 indicate a previously unknown mixture effect on hepatic gene expression. Considering the rapidly increasing use of e-cigarettes, this observation warrants further investigation.

## Acknowledgments

This work was supported by the National Institutes of Health National Institute of Environmental Health Sciences [Grants R01 ES017425,P42 ES04699, P01 ES011269] and by the United States Environmental Protection Agency [grant R833292]. Its contents are solely the responsibility of the grantee and do not necessarily represent the official views of the agency that provided the grant. Furthermore the grant agencies do not endorse the purchase of any commercial products or services mentioned in the

publication. We thank Jaya Bharati Muvvala (UC Davis) for her technical assistance with qPCR, Dr. Stelvio Bandiera (University of British Columbia) for generously providing the rabbit polyclonal anti-CYP2B1/2 antibody, and Dr. Xueshu Li (The University of Iowa) for recording the NMR spectra of the nicotine salt. We also thank Dr. Kim Keil, Dr. Adrienne Bautista and Mr. Hao Chen (UC Davis) for providing critical feedback on early drafts of the manuscript.

## Appendix A. Supplementary data

Supplementary data associated with this article can be found, in the online version, at http://dx.doi.org/10.1016/j.tox.2015.10.002.

## References


Anandatheerthavarada, H.K., Williams, J.F., Wecker, L., 1993a. The chronic administration of nicotine induces cytochrome p450 in rat brain. J. Neurochem. 60, 1941–1944.

Anandatheerthavarada, H.K., Williams, J.F., Wecker, L., 1993b. Differential effect of chronic nicotine administration on brain cytochrome p4501a1/2 and p4502e1. Biochem. Biophys. Res. Commun. 194, 312–318. doi:http://dx.doi.org/10.1006/bbrc.1993.1821.

Ariyoshi, N., Oguri, K., Koga, N., Yoshimura, H., Funae, Y., 1995. Metabolism of highly persistent pcb congener, 2,4,5,2,4,5-hexachlorobiphenyl, by human cyp2b6. Biochem. Biophys. Res. Commun. 212, 455–460. doi:http://dx.doi.org/10.1006/bbrc.1995.1991.

Birnbaum, L.S., 1983. Distribution and excretion of 2,3,6,2',3',6'- and 2,4,5,2',4',5'-hexachlorobiphenyl in senescent rats. Toxicol. Appl. Pharmacol. 70, 262–272.

Collins, B.C., Miller, C.A., Sposny, A., Hewitt, P., Wells, M., Gallagher, W.M., Pennington, S.R., 2012. Development of a pharmaceutical hepatotoxicity biomarker panel using a discovery to targeted proteomics approach. Mol. Cell. Proteomics 11, 394–410. doi:http://dx.doi.org/10.1074/mcp.M111.016493.

Crane, A.L., Klein, K., Zanger, U.M., Olson, J.R., 2012. Effect of cyp2b6*6 and cyp2c19*2 genotype on chlorpyrifos metabolism. Toxicology 293, 115–122. doi:http://dx.doi.org/10.1016/j.tox.2012.01.006.

Curran, C.P., Nebert, D.W., Genter, M.B., Patel, K.V., Schaefer, T.L., Skelton, M.R., Williams, M.T., Vorhees, C.V., 2011. In utero and lactational exposure to pcbs in mice: adult offspring show altered learning and memory depending on cyp1a2 and ahr genotypes. Environ. Health Perspect. 119, 1286–1293. doi:http://dx.doi.org/10.1289/ehp.1002965.

Czekaj, P., Wiaderkiewicz, A., Florek, E., Wiaderkiewicz, R., 2000. Expression of cytochrome cyp2b1/2 in nonpregnant, pregnant and fetal rats exposed to tobacco smoke. Acta Biochim. Pol. 47, 1115–1127.

Dannan, G.A., Guengerich, F.P., Kaminsky, L.S., Aust, S.D., 1983. Regulation of cytochrome p-450. Immunochemical quantitation of eight isozymes in liver microsomes of rats treated with polybrominated biphenyl congeners. J. Biol. Chem. 258, 1282–1288.

Dutheil, F., Jacob, A., Dauchy, S., Beaune, P., Scherrmann, J.M., Decleves, X., Loriot, M. A., 2010. Abc transporters and cytochromes p450 in the human central nervous system: influence on brain pharmacokinetics and contribution to neurodegenerative disorders. Expert Opin. Drug Metab. Toxicol. 6, 1161–1174. doi:http://dx.doi.org/10.1517/17425255.2010.510832.

Feo, M.L., Gross, M.S., McGarrigle, B.P., Eljarrat, E., Barceló, D., Aga, D.S., Olson, J.R., 2012. Biotransformation of bde-47 to potentially toxic metabolites is predominantly mediated by human cyp2b6. Environ. Health Perspect. 121, 440–446.

Fitzgerald, E.F., Hwang, S.-A., Lambert, G., Gomez, M., Tarbell, A., 2005. Pcb exposure and in vivo cyp1a2 activity among native americans. Environ. Health Perspect. 113, 272–277. doi:http://dx.doi.org/10.2307/3436039.

Foxenberg, R.J., Ellison, C.A., Knaak, J.B., Ma, C., Olson, J.R., 2011. Cytochrome p450-specific human pbpk/pd models for the organophosphorus pesticides: chlorpyrifos and parathion. Toxicology 285, 57–66. doi:http://dx.doi.org/10.1016/j.tox.2011.04.002.

Gahrs, M., Roos, R., Andersson, P.L., Schrenk, D., 2013. Role of the nuclear xenobiotic receptors car and pxr in induction of cytochromes p450 by non-dioxinlike polychlorinated biphenyls in cultured rat hepatocytes. Toxicol. Appl. Pharmacol. 272, 77–85. doi:http://dx.doi.org/10.1016/j.taap.2013.05.034.

Hrycay, E.G., Bandiera, S.M., 2003. Spectral interactions of tetrachlorobiphenyls with hepatic microsomal cytochrome p450 enzymes. Chem. Biol. Interact. 146, 285–296.

Hukkanen, J., Jacob 3rd, P., Peng, M., Dempsey, D., Benowitz, N.L., 2011. Effect of nicotine on cytochrome p450 1a2 activity. Br. J. Clin. Pharmacol. 72, 836–838. doi:http://dx.doi.org/10.1111/j.1365-2125.2011.04023.x.

Joshi, S.N., Vyas, S.M., Duffel, M.W., Parkin, S., Lehmler, H.J., 2011. Synthesis of sterically hindered polychlorinated biphenyl derivatives. Synthesis 2011, 1045–1054. doi:http://dx.doi.org/10.1055/s-0030-1258454.

Kania-Korwel, I., Barnhart, C.D., Stamou, M., Truong, K.M., El-Komy, M.H.M.E., Lein, P. J., Veng-Pedersen, P., 2012. 2,2′,3,5′,6-pentachlorobiphenyl (pcb 95) and its hydroxylated metabolites are enantiomerically enriched in female mice. Environ. Sci. Technol. 46, 11393–11401. doi:http://dx.doi.org/10.1021/es302810t.

Kania-Korwel, I., Lehmler, H.J., 2015. Chiral polychlorinated biphenyls: absorption, metabolism and excretion – a review. Environ. Sci. Pollut. Res. Int. doi:http://dx.doi.org/10.1007/s11356-015-4150-2.

Kania-Korwel, I., Shaikh, N.S., Hornbuckle, K.C., Robertson, L.W., Lehmler, H.-J., 2007. Enantioselective disposition of pcb 136 (2,2,3,3,6,6-hexachlorobiphenyl) in c57bl/6 mice after oral and intraperitoneal administration. Chirality 19, 56–66. doi:http://dx.doi.org/10.1002/chir.20342.

Kania-Korwel, I., Vyas, S.M., Song, Y., Lehmler, H.-J., 2008. Gas chromatographic separation of methoxylated polychlorinated biphenyl atropisomers. J. Chromatogr. A 1207, 146–154. doi:http://dx.doi.org/10.1016/j.chroma.2008.08.044.

Khokhar, J.Y., Miksys, S.L., Tyndale, R.F., 2010. Rat brain cyp2b induction by nicotine is persistent and does not involve nicotinic acetylcholine receptors. Brain Res. 1348, 1–9. doi:http://dx.doi.org/10.1016/j.brainres.2010.06.035.

Khokhar, J.Y., Tyndale, R.F., 2011. Drug metabolism within the brain changes drug response: selective manipulation of brain cyp2b alters propofol effects. Neuropsychopharmacology 36, 692–700. doi:http://dx.doi.org/10.1038/npp.2010.202.

Kim, K.H., Bose, D.D., Ghogha, A., Riehl, J., Zhang, R., Barnhart, C.D., Lein, P.J., Pessah, I. N., 2011. Para- and ortho-substitutions are key determinants of polybrominated diphenyl ether activity toward ryanodine receptors and neurotoxicity. Environ. Health Perspect. 119, 519–526. doi:http://dx.doi.org/10.1289/ehp.1002728.

Kozul, C.D., Nomikos, A.P., Hampton, T.H., Warnke, L.A., Gosse, J.A., Davey, J.C., Thorpe, J.E., Jackson, B.P., Ihnat, M.A., Hamilton, J.W., 2008. Laboratory diet profoundly alters gene expression and confounds genomic analysis in mouse liver and lung. Chem. Biol. Interact. 173, 129–140. doi:http://dx.doi.org/10.1016/j.cbi.2008.02.008.

Le Houezec, J., Jacob 3rd, P., Benowitz, N.L., 1993. A clinical pharmacological study of subcutaneous nicotine. Eur. J. Clin. Pharmacol. 44, 225–230.

Lee, S., Busby, A.L., Timchalk, C., Poet, T.S., 2008. Effects of nicotine exposure on in vitro metabolism of chlorpyrifos in male sprague-dawley rats. J. Toxicol. Environ. Health Part A 72, 74–82. doi:http://dx.doi.org/10.1080/15287390802477288.

Lehmler, H.-J., Harrad, S.J., Huhnerfuss, H., Kania-Korwel, I., Lee, C.M., Lu, Z., Wong, C. S., 2010. Chiral polychlorinated biphenyl transport, metabolism, and distribution: a review. Environ. Sci. Technol. 44, 2757–2766. doi:http://dx.doi.org/10.1021/es902208u.

Lu, Z., Kania-Korwel, I., Lehmler, H.J., Wong, C.S., 2013. Stereoselective formation of mono- and dihydroxylated polychlorinated biphenyls by rat cytochrome p450 2b1. Environ. Sci. Technol. 47, 12184–12192. doi:http://dx.doi.org/10.1021/es402838f.

Matta, S.G., Balfour, D.J., Benowitz, N.L., Boyd, R.T., Buccafusco, J.J., Caggiula, A.R., Craig, C.R., Collins, A.C., Damaj, M.I., Donny, E.C., Gardiner, P.S., Grady, S.R., Heberlein, U., Leonard, S.S., Levin, E.D., Lukas, R.J., Markou, A., Marks, M.J., McCallum, S.E., Parameswaran, N., Perkins, K.A., Picciotto, M.R., Quik, M., Rose, J. E., Rothenfluh, A., Schafer, W.R., Stolerman, I.P., Tyndale, R.F., Wehner, J.M., Zirger, J.M., 2007. Guidelines on nicotine dose selection for in vivo research. Psychopharmacology (Berl) 190, 269–319.

Meyer, R.P., Gehlhaus, M., Knoth, R., Volk, B., 2007. Expression and function of cytochrome p450 in brain drug metabolism. Curr. Drug Metab. 8, 297–306.

Miksys, S., Hoffmann, E., Tyndale, R.F., 2000. Regional and cellular induction of nicotine-metabolizing cyp2b1 in rat brain by chronic nicotine treatment. Biochem. Pharmacol. 59, 1501–1511. doi:http://dx.doi.org/10.1016/s0006-2952(00)00281-1.

Miksys, S., Lerman, C., Shields, P.G., Mash, D.C., Tyndale, R.F., 2003. Smoking, alcoholism and genetic polymorphisms alter cyp2b6 levels in human brain. Neuropharmacology 45, 122–132.

Miksys, S., Tyndale, R.F., 2013. ccnp heinz lehmann award paper: cytochrome p450-mediated drug metabolism in the brain. J. Psychiatry Neurosci. 38, 152–163. doi:http://dx.doi.org/10.1503/jpn.120133.

Niknam, Y., Feng, W., Cherednichenko, G., Dong, Y., Joshi, S.N., Vyas, S.M., Lehmler, H.-J., Pessah, I.N., 2013. Structure-activity relationship of select meta- and para-hydroxylated non-dioxin-like polychlorinated biphenyls: from single ryr1 channels to muscle dysfunction. Toxicol. Sci. 136, 500–513.

Noel, J.K., Rees, V.W., Connolly, G.N., 2011. Electronic cigarettes: a new 'tobacco' industry? Tob. Control 20, 81. doi:http://dx.doi.org/10.1136/tc.2010.038562.

Panesar, S.K., Bandiera, S.M., Abbott, F.S., 1996. Comparative effects of carbamazepine and carbamazepine-10,11-epoxide on hepatic cytochromes p450 in the rat. Drug Metab. Dispos. 24, 619–627.

Pessah, I.N., Cherednichenko, G., Lein, P.J., 2010. Minding the calcium store: ryanodine receptor activation as a convergent mechanism of pcb toxicity. Pharmacol. Ther. 125, 260–285. doi:http://dx.doi.org/10.1016/j.pharmthera.2009.10.009.

Pessah, I.N., Lehmler, H.-J., Robertson, L.W., Perez, C.F., Cabrales, E., Bose, D.D., Feng, W., 2009. Enantiomeric specificity of (−)-2,2',3,3',6,6'-hexachlorobiphenyl toward ryanodine receptor types 1 and 2. Chem. Res. Toxicol. 22, 201–207.

Pfaffl, M.W., 2001. A new mathematical model for relative quantification in real-time rt–pcr. Nucleic Acids Res. 29, e45. doi:http://dx.doi.org/10.1093/nar/29.9.e45.

Price, R.J., Renwick, A.B., Walters, D.G., Young, P.J., Lake, B.G., 2004. Metabolism of nicotine and induction of cyp1a forms in precision-cut rat liver and lung slices. Toxicol. In Vitro 18, 179–185.

Regan, A.K., Promoff, G., Dube, S.R., Arrazola, R., 2013. Electronic nicotine delivery systems: adult use and awareness of the 'e-cigarette' in the USA. Tob. Control 22, 19–23. doi:http://dx.doi.org/10.1136/tobaccocontrol-2011-050044.

Ronis, M.J., Rowlands, J.C., Hakkak, R., Badger, T.M., 1999. Altered expression and glucocorticoid-inducibility of hepatic cyp3a and cyp2b enzymes in male rats fed diets containing soy protein isolate. J. Nutr. 129, 1958–1965.

Siemens, N., Patenge, N., Otto, J., Fiedler, T., Kreikemeyer, B., 2011. Streptococcus pyogenes m49 plasminogen/plasmin binding facilitates keratinocyte invasion via integrin-integrin-linked kinase (ilk) pathways and protects from macrophage killing. J. Biol. Chem. 286, 21612–21622. doi:http://dx.doi.org/10.1074/jbc.M110.202671.

Stamou, M., Wu, X., Kania-Korwel, I., Lehmler, H.J., Lein, P.J., 2014. Cytochrome p450 mrna expression in the rodent brain: species-, sex-, and region-dependent differences. Drug Metab. Dispos. 42, 239–244. doi:http://dx.doi.org/10.1124/dmd.113.054239.

Tian, N., Arany, I., Waxman, D.J., Baliga, R., 2010. Cytochrome-p450 2b1 gene silencing attenuates puromycin aminonucleoside-induced cytotoxicity in glomerular epithelial cells. Kidney Int. 78, 182–190. doi:http://dx.doi.org/10.1038/ki.2010.100.

Twaroski, T.P., O'Brien, M.L., Larmonier, N., Glauert, H.P., Robertson, L.W., 2001. Polychlorinated biphenyl-induced effects on metabolic enzymes, ap-1 binding, vitamin e, and oxidative stress in the rat liver. Toxicol. Appl. Pharmacol. 171, 85–93. doi:http://dx.doi.org/10.1006/taap.2000.9114.

Warner, N.A., Martin, J.W., Wong, C.S., 2008. Chiral polychlorinated biphenyls are biotransformed enantioselectively by mammalian cytochrome p-450 isozymes to form hydroxylated metabolites. Environ. Sci. Technol. 43, 114–121. doi:http://dx.doi.org/10.1021/es802237u.

Wu, X., Kania-Korwel, I., Chen, H., Stamou, M., Dammanahalli, K.J., Duffel, M., Lein, P.J., Lehmler, H.J., 2013. Metabolism of 2,2',3,3',6,6'-hexachlorobiphenyl (pcb 136) atropisomers in tissue slices from phenobarbital or dexamethasone-induced rats is sex-dependent. Xenobiotica 43, 933–947. doi:http://dx.doi.org/10.3109/00498254.2013.785626.

Wu, X., Pramanik, A., Duffel, M.W., Hrycay, E.G., Bandiera, S.M., Lehmler, H.J., Kania-Korwel, I., 2011. 2,2',3,3',6,6'-hexachlorobiphenyl (pcb 136) is enantioselectively oxidized to hydroxylated metabolites by rat liver microsomes. Chem. Res. Toxicol. 24, 2249–2257. doi:http://dx.doi.org/10.1021/tx200360m.

Yamin, C.K., Bitton, A., Bates, D.W., 2010. E-cigarettes: a rapidly growing internet phenomenon. Ann. Intern. Med. 153, 607–609. doi:http://dx.doi.org/10.7326/0003-4819-153-9-201011020-00011.

Yang, D., Kania-Korwel, I., Ghogha, A., Chen, H., Stamou, M., Bose, D.D., Pessah, I.N., Lehmler, H.J., Lein, P.J., 2014. Pcb 136 atropselectively alters morphometric and functional parameters of neuronal connectivity in cultured rat hippocampal neurons via ryanodine receptor-dependent mechanisms. Toxicol. Sci. 138, 379–392. doi:http://dx.doi.org/10.1093/toxsci/kft334.

Zhou, S.F., Wang, B., Yang, L.P., Liu, J.P., 2010. Structure, function, regulation and polymorphism and the clinical significance of human cytochrome p450 1a2. Drug Metab. Rev. 42, 268–354. doi:http://dx.doi.org/10.3109/03602530903286476.